5.5. Comparison between models for heterogeneous and homogeneous systems.
For homogeneous reaction systems, the well-known Hatta number Ha is defined as:

$$Ha_n = (1/k_L)\{2k_n C_{Ai}^{n-1} C_B^m D/(n+1)\}^{\frac{1}{2}} \qquad (5\text{-}123)$$

In Table 5.1. expressions of Ha and Θ are presented for correlation.

Table 5.1. Correlation of the dimensionless physical quantities Ha and Θ for homogeneous and heterogeneous chemical reactions of zero order and first order in gas component A.

	Homogeneous reaction	Heterogeneously catalyzed reaction
n = 0	$Ha_o = (1/k_L)(2k_o C_B^m D/C_{Ai})^{\frac{1}{2}}$	$\Theta_o = (1/k_L)(2k_o C_B^m D\phi/C_{Ai})^{\frac{1}{2}} = Ha_o\phi^{\frac{1}{2}}$
n = 1	$Ha_1 = (1/k_L)(k_1 C_B^m D)^{\frac{1}{2}}$	$\Theta_1 = (1/k_L)(k_1 C_B^m D\phi)^{\frac{1}{2}} = Ha_1\phi^{\frac{1}{2}}$

It is well-known from the theory of homogeneous chemical reactions that for $Ha > 2$ and $C_B/C_A \gg 1$:

$$E = Ha \qquad (5\text{-}124)$$

which means that in the case that the catalyst particles are distributed homogeneously in both liquid film and bulk of the liquid:

$$E = Ha(\phi'')^{\frac{1}{2}} \qquad (5\text{-}125)$$

In the case that the catalyst particles are assumed to be in the liquid film only, eqn (5-125) is changed into:

$$E = Ha\phi^{\frac{1}{2}} \qquad (5\text{-}126)$$

Further, it can be noted that an enhancement factor $E < 1$ is obtained if the catalyst particles are distributed in the bulk of the liquid only.

5.6. Summary.
In this chapter we developed three models for describing mass transfer of a component from a gas phase to the active sites of a solid catalyst particle suspended in a liquid.
In the first model, the catalyst particles are distributed homogeneously in the bulk of the liquid only. The enhancement factor never exceeds unity. This model can be applied if the catalyst particles are large e.g. $d_p > \delta$ and $d_p > d_s$.
In the second model it was assumed that the catalyst particles are distributed homogeneously in the liquid film only. This model can be applied if the catalyst particles are small relative to the thickness of the liquid film e.g. $d_p < \delta$ and $d_p < 0.025\ d_s$. The enhancement factor can be considerably larger than unity.
In the third model, the catalyst particles are distributed homogeneously in both liquid film and bulk of the liquid. The catalyst particles are small relative to the thickness of the liquid film and the enhancement factor can be larger than unity.
Further, in Table 5.1. we showed that the Ha-number for a homogeneous chemical reaction and Θ for a heterogeneous chemical reaction can be correlated.

Table 5.2. Survey of models for calculation of the enhancement factor of gas absorption of heterogeneously catalyzed chemical reactions.

Model 1 catalyst particles in the bulk of the liquid only

$n = 0$

$\eta_o = 1$ $\quad E = \frac{1}{2}\Theta_o^2/(1 - a_L\delta)$ (5-9)

$\eta_o < 1$ $\quad E(1 + 1/\Gamma' - 4(1 - a_L\delta)\Lambda_o/\Theta_o^2) - 3\Lambda_o\{(1 - 2(1 - a_L\delta)E/\Theta_o^2)^{2/3} - 1\} = 1$ (5-28)

$n = 1$ $\quad 1/E = 1 + (1 - a_L\delta)\Lambda_1\{\Theta_1^2(((3\Lambda_1)^{\frac{1}{2}})\coth((3\Lambda_1)^{\frac{1}{2}}) - 1)\}^{-1} + 1/\Gamma'$ (5-46)

Model 2 catalyst particles in the liquid film only

$n = 0$

$E < 2$ $\quad E = \frac{1}{2}\Theta_o^2$ (5-56)

$E > 2$ $\quad E = \Theta_o$ (5-66)

$n = 1$ $\quad E = \Theta_1\tanh(\Theta_1) \simeq \Theta_1$ for large values of Θ_1 e.g. $\Theta_1 > 2$ (5-76)

Model 3 catalyst particles in both liquid film and bulk of the liquid

$n = 0$ $\quad E < 2$ and $\eta_o = 1$

$E = \frac{1}{2}\Theta_o^2$ (5-82)

$E < 2$ and $\eta_o < 1$

$\frac{1}{2}\Theta_o^2\{(2E/\Theta_o^2 - a_L\delta)(1/\Gamma + 1 - a_L\delta)/(1 - a_L\delta) + \frac{1}{2}a_L\delta\} +$

$+ \Lambda_o\{1 - 3(1 + (a_L\delta - 2E/\Theta_o^2)/(1 - a_L\delta))^{2/3} +$ (5-94)

$+ 2(1 + (a_L\delta - 2E/\Theta_o^2)/(1 - a_L\delta))\} = 1$

$E > 2$

$E = (a_L\delta)^{\frac{1}{2}}\Theta_o$ (5-104)

$n = 1$ $\quad E < 2$

$E = (\lambda''\delta)\tanh(\lambda''\delta) +$ (5-115)

$\eta_1\Theta_1^2(1 - a_L\delta)/(\cosh^2(\lambda''\delta))\{(\eta_1\Theta_1^2(1 - a_L\delta)/(\lambda''\delta))\tanh(\lambda''\delta) + 1 +$

$+ \eta_1\Theta_1^2/\Gamma\}^{-1}$

in which $\lambda''\delta = (a_L\delta)^{\frac{1}{2}}\Theta_1$ (5-116)

$E > 2$

$E = (\lambda''\delta)\tanh(\lambda''\delta)$ (5-122)

For each model presented in Table 5.2. it is assumed that:
- the catalyst particles are spherical;
- the active sites are distributed homogeneously in the catalyst particle;
- there is no resistance to mass transfer in the gas phase;
- for the component B and the product(s), there is no resistance to mass transfer, neither in the liquid nor in the pores of the catalyst particles;
- the solubility of the gas in the liquid C_{Ai} as well as the mass transfer coefficient k_L are not affected by the concentration of the catalyst.

The models represented in Table 5.2. deal with catalyst particles homogeneously distributed in:
- the bulk of the liquid only;
- the liquid film only;
- both the liquid film and the bulk of the liquid.

CHAPTER 6

GAS ABSORPTION EXPERIMENTS WITH A THREE-PHASE REACTION SYSTEM

6.1. Introduction.

In this chapter, the results are presented of gas absorption experiments with some three-phase reaction systems in a Whitman cell of about 1 litre. The gas absorption rate has been determined with and without chemical reaction i.e. with and without addition of catalyst particles to the liquid in the reactor. The reactions studied were the hydrogenation of:
- hydroxylamine to ammonia and water in an aqueous solution;
- 3-pentanone to 3-pentanol in aqueous solution;
- styrene to ethylbenzene in n-heptane.

The rates of gas absorption with and without chemical reaction have been determined in the Whitman cell under identical conditions with respect to temperature, stirrer speeds and specific interfacial area.

6.2. Equipment.

The measurements were performed in a closed cylindrical glass reactor as shown in Fig. 6.1. The reactor was provided with a thermostatted jacket all round to make sure that the gas absorption and the chemical reaction occurred at a fixed temperature. The inside diameter was about 11 cm; the height about 16 cm. The total volume of the Whitman cell was about 1.5 litres; the cell had a liquid content of about 1 litre. Gas phase and liquid phase were stirred separately with magnetic stirrers. The gas phase was stirred with a flat stirrer N with a speed of 7.75 s^{-1}. The liquid phase was stirred with a tulip stirrer G with a speed of 12.5 s^{-1}. The reactor was equipped with four baffles F. The experiments were carried out at atmospheric pressure and at temperatures of 30 and 40 ^{o}C. The pressure in the reactor was controlled by means of a manometer H filled with solvent. One leg of the manometer was connected to the gas phase of the reactor, the other to the surrounding atmosphere.
Due to the absorption of gas from the gas phase into the liquid phase, the pressure in the reactor would decrease if the volume of the gas phase remained unchanged. However, during the gas absorption the pressure was kept constant by decreasing the volume of the gas phase with a plunger P. This was done by turning the thimble of the micrometer S of the measuring equipment E in such a way that the liquid level in the manometer remained unchanged.
Assuming that during the time Δt a displacement $\Delta \ell$ of the plunger is reached, the rate of gas absorption can be calculated from:

$$\Phi_A = (P_t - P_v)\pi d_i^2 \Delta \ell / (4\tilde{R}T\Delta t V_L) \qquad (6\text{-}1)$$

Through an inlet B in the liquid phase degassed solvent could be fed to the Whitman cell to perform experiments for the determination of mass transfer coefficients.
Gas could be supplied to the cell through inlet D and vented through outlet M.
The temperature was read by means of a HP-2802A thermometer equipped with a 100 Ω Pt-resistance probe, type 18643A. The accuracy of this apparatus is within ± 0.5 K. The resolution is 0.01 K. The probe C was placed in the liquid.
The specific interfacial area was about 10 m^{-1}.

6.3. Measurement of mass transfer coefficient.

6.3.1. Procedure.

About 1.5 litres of liquid were degassed in a separate vessel for about 3 hours at room temperature by means of a vacuum pump. During degassing, the liquid was stirred continuously. About 10 ml of the degassed liquid was brought into the

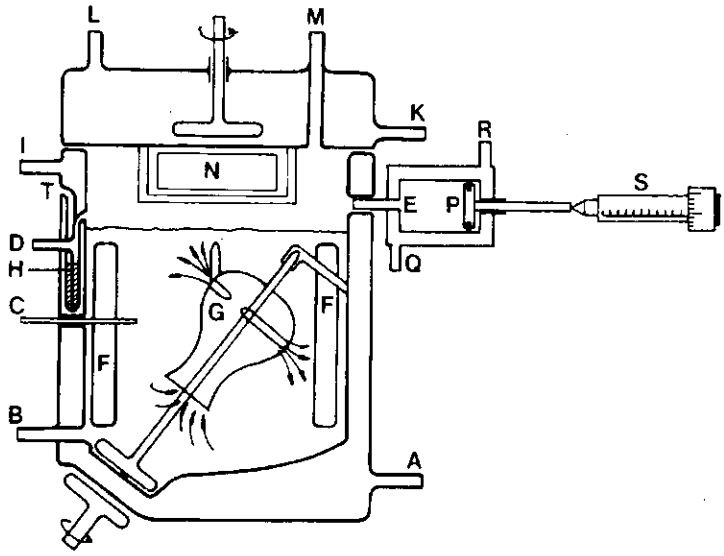

Fig. 6.1. Whitman cell for performing gas absorption rate experiments.

A. Water from thermostat
B. Degassed solvent inlet
C. Pt-100 thermometer
D. Gas inlet
E. Measuring equipment
F. Baffles
G. Liquid stirrer
H. Manometer
I. Water to thermostat
K. Water from thermostat
L. Water to thermostat
M. Gas outlet
N. Gas stirrer
P. Plunger
Q. Water from thermostat
R. Water to thermostat
S. Micrometer
T. Outlet of manometer

Whitman cell, after which the cell was closed. The reactor was accurately checked for leakage by means of the manometer and both stirrers were started. The reactor was purged with five times its volume of nitrogen. After this, hydrogen was led into the reactor to an amount of seven times the reactor volume. After purging with this amount of hydrogen, the stopcocks were closed and the operating conditions of the reactor were adjusted to the required temperature, pressure and speed of stirrers. Due to the presence of some liquid in the cell, the hydrogen was already saturated with solvent vapour.
When the required experimental conditions had been reached, the liquid-phase stirrer was stopped and the degassed liquid was brought into the reactor after passing a heat exchanger to obtain the required temperature before entering the cell. The cell was filled with liquid to about the same level in all experiments. During filling of the reactor with liquid, the excess of hydrogen was removed through the gas outlet M.
As soon as the reactor had been filled, the liquid inlet B and the gas outlet M were closed. The stopwatch and the liquid-phase stirrer were started at the same time. The displacement of the plunger was noted down every minute.
After the experiment was carried out, the liquid phase was weighed and the specific interfacial area calculated, using the known density of the liquid.

6.3.2. Calculation of mass transfer coefficient.
The absorption rate of gas into the liquid is given by:

$$\Phi_A(t) = k_L a_L (C_{Ai} - C_A(t)) = dC_A(t)/dt \qquad (6\text{-}2)$$

Solving of the differential equation leads to:

$$\ln(C_{Ai} - C_A(t)) = - k_L a_L t + C_{13} \qquad (6\text{-}3)$$

For $t = 0$ it is supposed that $C_A = C_A^o$ so that:

$$\ln(C_{Ai} - C_A(t)) = - k_L a_L t + \ln(C_{Ai} - C_A^o) \qquad (6\text{-}4)$$

From eqn (6-2) one finds:

$$\ln(\Phi_A(t)) = \ln(k_L a_L) + \ln(C_{Ai} - C_A(t)) \qquad (6\text{-}5)$$

Substitution of eqn (6-5) into eqn (6-4) yields:

$$\ln(\Phi_A(t)) = \ln(k_L a_L) + \ln(C_{Ai} - C_A^o) - k_L a_L t = C_{14} - k_L a_L t \qquad (6\text{-}6)$$

A plot of $\ln(\Phi_A(t))$ versus t gives a straight line whose slope b is equal to $-k_L a_L$.
The specific interfacial area is calculated from the mass of liquid M_L, the density ρ_L and the liquid surface area $\pi D_w^2/4$ so that:

$$k_L = -4bM_L/(\pi D_w^2 \rho_L) \qquad (6\text{-}7)$$

6.4. Measurement of gas absorption rates with chemical reaction.

6.4.1. Procedure.
About 1.5 litres of solvent were in a separate vessel degassed for about 3 hours at room temperature by means of a vacuum pump under constant stirring.
The catalyst was put into a small vessel together with about 100 ml of solvent and saturated with hydrogen under constant bubbling, for about 1 hour.
The procedures of filling the reactor and starting the reaction were different for the three reaction systems used.
For the hydrogenation of hydroxylamine, the aqueous solution of hydroxylamine phosphate was first prepared, after which a pH = 5 was obtained by addition of KH_2PO_4.
The aqueous solution was brought into the reactor, after which immediately the catalyst was added to the liquid phase. After closing of the cell, the gas-phase stirrer was started and the gas space was purged with about five times its volume of nitrogen. The nitrogen was removed completely by purging the gas space with about seven times its volume of hydrogen.
The measuring equipment E was rinsed too with hydrogen by moving the plunger up and down several times.
After closing of both the gas inlet D and the gas outlet M, the gas phase was saturated with water vapour.
This process was followed by means of manometer H. When the pressure in the reactor did not increase anymore, the stopwatch and the liquid stirrer were started.
For the hydrogenation of 3-pentanone in water, the reactor was first filled with degassed water and catalyst. The reactor was closed and the gas phase was purged with nitrogen and hydrogen as described above.
After closing of the inlet D and the outlet M, the liquid stirrer was started and the gas phase was saturated with water vapour.
When the gas phase was saturated, 13 g of 3-pentanone was injected into the

liquid phase through a septum placed in inlet B, and the stopwatch was started.
For the hydrogenation of styrene in n-heptane we made use of a large glass syringe of 150 ml, which was thermostatted. The syringe was filled with a fifty-fifty mixture of styrene and n-heptane and connected to the inlet B.
Then the reactor was filled with the required amount of n-heptane and catalyst. The gas space was purged with nitrogen and next with hydrogen as described above and the gas inlet D and gas outlet M were closed.
When the gas phase was saturated with solvent vapour, the mixture of styrene and n-heptane was injected from the 150 ml syringe into the liquid phase of the reactor through inlet B by pushing the plunger. The excess of hydrogen was removed through gas outlet M. When inlet B and outlet M were closed, the stopwatch was started.

6.4.2. Calculation of gas absorption rate.
The measurement of the gas absorption rate was performed by reading the absorbed volume of gas each minute under steady-state conditions i.e. constant pressure, constant gas phase composition and constant values of stirrer speed, specific interfacial area and temperature.
The gas absorption rate is found from the displacement of the plunger P necessary to maintain a constant pressure in the cell.
The gas absorption rate is calculated from:

$$\Phi_A = (P_t - P_v)\pi d_i^2 \Delta l/(4\tilde{R}T\Delta t V_L) \qquad (6\text{-}8)$$

6.5. Experimental results.

6.5.1. Hydrogenation of hydroxylamine in water.
The hydrogenation of hydroxylamine in water has been discussed extensively by Van de Moesdijk [112]. In an acid medium the reaction can be described by the equation:

$$NH_3^+OH\ (aq) + H_2\ (aq) = NH_4^+\ (aq) + H_2O\ (l) \qquad (6\text{-}9)$$

This reaction may be considered of zero order with respect to hydrogen partial pressure at pH = 5 and $p_{H_2} > 0.5$ bar. The reaction rate is highly pH-dependent and increases with increasing pH. In an acid medium the reaction can be described by an apparent order of a half with respect to C_B, the total hydroxylamine concentration. The reaction rate was found to be directly proportional to the catalyst concentration in the range of 0 - 10 kg m^{-3}.
Since by the chemical reaction ammonia is produced and the reaction rate is highly pH-dependent, the aqueous solution is buffered with KH_2PO_4.
The hydrogenation was carried out in aqueous solutions containing 1113 g of demineralized water, 0.745 g of hydroxylamine orthophosphate and 46.3 g of KH_2PO_4. The total mass of the liquid phase was about 1160 g. The density of the solution was 1023 kg m^{-3} at 40 °C. The volume of liquid in the reactor was 1134 cm^3, which gives an interfacial area of 8.7 m^{-1} in the Whitman cell with inside diameter 11 cm. The experiments were performed at 40 °C and pH = 5.
As catalyst we used a 10 wt % Pd/C catalyst from Fluka. The particle diameter distribution is given in Fig. 6.2.
The number-average particle diameter is 4.0 μm. The density of the porous particles is 405 kg m^{-3}, whereas the density of the solid itself is 2023 kg m^{-3}, resulting in a porosity of 0.80. The pores volume is 2 10^{-3} m^3 kg^{-1}.
The specific surface area of this catalyst is 766 10^3 m^2 kg^{-1}.
In Table 6.1., these values are summarized.

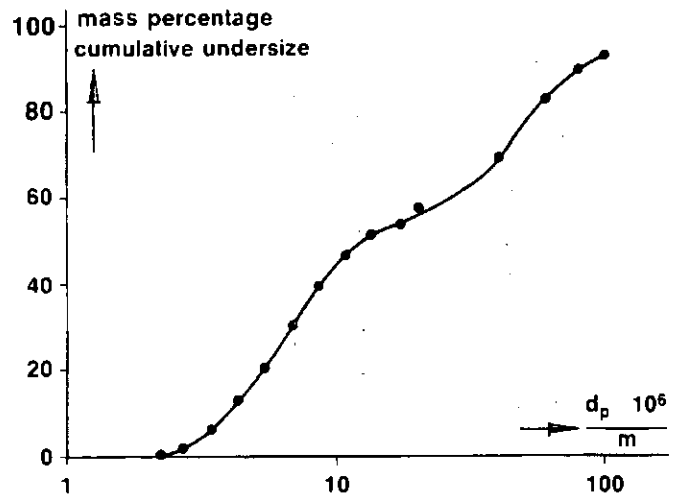

Fig. 6.2. Catalyst particle diameter distribution of 10 wt % Pd/C from Fluka.

Table 6.1. Properties of the 10 wt % Pd/C catalyst from Fluka.

d_p = 4.0 μm	V_p = 2 10^{-3} m^3 kg^{-1}
ρ_p = 405 kg m^{-3}	S_p = 766 10^3 m^2 kg^{-1}
ρ_s = 2023 kg m^{-3}	δ_p = 10 nm
ε_p = 0.80	

For the liquid-film mass transfer coefficient we found a value of 4.9 10^{-5} m s^{-1}. In Chapters 3 and 4, for the solubility and the diffusion coefficient of hydrogen in the above-described solution we obtained C_{Ai} = 0.58 mol m^{-3} and D = 4.2 10^{-9} m^2 s^{-1} respectively; both values refer to 40 °C and a total pressure of 1 bar.
For the effective diffusion coefficient of hydrogen in the pores of the catalyst particles we used a value of 1.1 10^{-9} m^2 s^{-1}. This value was calculated from the relation $D^* = D\varepsilon_p/\tau$ in which ε_p = 0.8 and τ = 3 for carbon particles [119].
In Table 6.2. we have summarized the data with which we have made our calculations.

Table 6.2. Properties of the system hydrogen/aqueous hydroxylamine solution at 40 °C and at about 1 bar total pressure in the Whitman cell.

k_L = 4.9 10^{-5} m s^{-1}	C_{Ai} = 0.58 mol m^{-3}
D = 4.2 10^{-9} m^2 s^{-1}	a_L = 8.7 m^{-1}
D^* = 1.1 10^{-9} m^2 s^{-1}	

In Table 6.3. the experimental results of the hydrogenation of hydroxylamine in water are given. The enhancement factor has been calculated from $\Phi_A/(k_L a_L C_{Ai})$. From the data given, it is found that $a_L\delta = a_L D/k_L \approx 7\ 10^{-4}$. It is obvious that $\phi' = \phi''$ for this small value of $a_L\delta$.

Table 6.3. Experimental results of the hydrogenation of hydroxylamine in water at 40 °C and at about 1 bar total pressure.

Exp. No.	$\Phi_A\ 10^3$	E	$\overline{C}_p\ 10^3$	C_B	$\phi'\ 10^3$	ϕ	$\phi''\ 10^3$
	mol m^{-3} s^{-1}		kg m^{-3}	mol m^{-3}			
6-1	0.062	0.25	24	10	0.059	0.079	0.059
6-2	0.090	0.36	44	10	0.109	0.146	0.109
6-3	0.0111	0.43	58	10	0.143	0.192	0.143
6-4	0.0154	0.62	75	10	0.185	0.248	0.185
6-5	0.0190	0.77	88	10	0.217	0.291	0.217
6-6	0.0215	0.87	90	10	0.222	0.298	0.222

Model 1: reaction in the bulk of the liquid only.

From eqn (5-9) and Table 5.1., it is found that:

$$E = \tfrac{1}{2}\Theta_o^2/(1 - a_L\delta) = \tfrac{1}{2}Ha_o^2\phi/(1 - a_L\delta) \qquad (6\text{-}10)$$

After substitution of the values of Table 6.2. in eqn (5-123), we obtain:

$$Ha_o^2 = C_{15}\, k_o \qquad (6\text{-}11)$$

in which:

$$C_{15} = 19.1\ (\text{mol}\ m^{-3})^{-\frac{1}{2}}\ s \qquad (6\text{-}12)$$

so that:

$$E = C_{16}\, k_o \phi \qquad (6\text{-}13)$$

in which:

$$C_{16} = 9.5\ (\text{mol}\ m^{-3})^{-\frac{1}{2}}\ s \qquad (6\text{-}14)$$

From a plot of E versus ϕ it is found that:

$$k_o = 0.27\ (\text{mol}\ m^{-3})^{\frac{1}{2}}\ s^{-1} \qquad (6\text{-}15)$$

With this value of k_o the values of Θ_o^2, Γ' and A_o can be calculated. The results of these calculations are given in Table 6.4. For the calculation of Γ' we used $k_s = 2D/d_p = 2.1\ 10^{-3}$ m s^{-1} and $a_s = 6\overline{C}_p/(d_p\rho_p)$.
From Table 6.4. we may conclude that for all experiments the inequality of expression (5-19) was satisfied since $\Theta_o^2 < 2$. This means that for all experiments the effectiveness equals unity and that application of eqn (5-9) was correct. In Table 6.5., the experimental and calculated enhancement factors are compared.
A graphical comparison between E_{exp} and E_{calc} is made in Fig. 6.3.

Table 6.4. Calculated values of Θ_o^2, Γ' and Λ_o for k_o = 0.27 (mol m^{-3})$^{\frac{1}{2}}$ s^{-1}.

Exp. No.	Θ_o^2	Λ_o 10^3	Γ' 10^{-3}	$2(1 - \Lambda_o)(1 - a_L\delta)/(1/\Gamma' + 1)$
6-1	0.42	0.9	0.44	2
6-2	0.76	0.9	0.81	2
6-3	1.01	0.9	1.07	2
6-4	1.30	0.9	1.38	2
6-5	1.53	0.9	1.62	2
6-6	1.56	0.9	1.65	2

Table 6.5. Experimental and calculated enhancement factors for the hydrogenation of hydroxylamine in water at 40 °C and pH = 5 at a total pressure of about 1 bar.

Exp. No.	E_{exp}	E_{calc}	$\frac{1}{2}\Theta_o^2/(1 - a_L\delta)$
6-1	0.25	0.21	0.21
6-2	0.36	0.38	0.38
6-3	0.43	0.51	0.51
6-4	0.62	0.65	0.65
6-5	0.77	0.77	0.77
6-6	0.87	0.78	0.78

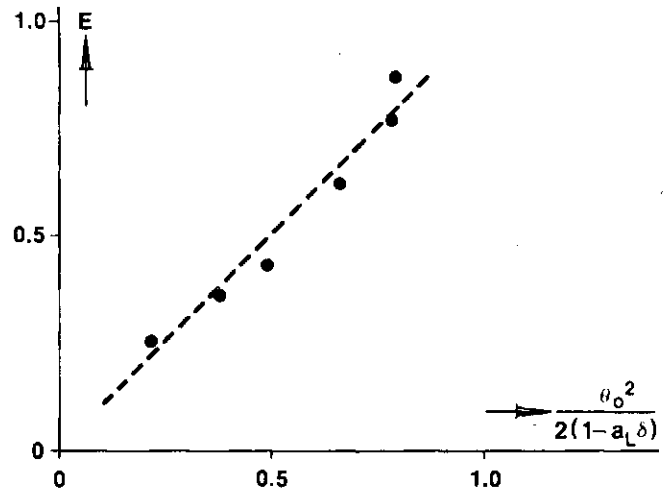

Fig. 6.3. Experimentally determined points and the calculated best-fit curve (eqn (6-10)) representing the enhancement factor as a function of $\frac{1}{2}\Theta_o^2/(1 - a_L\delta)$ for the hydrogenation of hydroxylamine in water at pH = 5 and T = 40 °C and at a total pressure of about 1 bar (Model 1).

Model 2: reaction in the liquid film only.

This model was not applied to the experiments of Table 6.3. since it was visually observed that the catalyst particles were not in the liquid film only. Experiments with higher gas absorption rates could not be carried out because the hydroxylamine would decompose into ammonia and dinitrogen oxide on the active sites of the catalyst particles if the concentration of hydrogen in the liquid was below a certain minimum value [112].

Model 3: reaction in the liquid film and in the bulk of the liquid.

From eqn (5-82) and Table 5.1., it is found that for $E \leq 2$ and $\tau_o = 1$:

$$E = \tfrac{1}{2}\Theta_o^2 = \tfrac{1}{2}Ha_o^2\Phi \qquad (6\text{-}16)$$

In our experiments in the Whitman cell, the value of $a_L\delta \ll 1$. As a consequence, the same relations and results can be expected as with Model 1.

Van de Moesdijk gives at pH = 5.0 a reaction rate constant of 10 $(\text{mmol } l^{-1})^{\frac{1}{2}}$ $(\text{g cat h})^{-1}$ at 60 °C for the reaction rate equation:

$$\Phi_A = k_o^* C_B^{\frac{1}{2}} \overline{C}_p \qquad (6\text{-}17)$$

The value of $k_o^* = k_o/\rho_p$ from our experiments at 40 °C equals:

$$k_o^* = 2.5 \ (\text{mmol } l^{-1})^{\frac{1}{2}} \ (\text{g cat h})^{-1} \qquad (6\text{-}18)$$

This result obtained at 40 °C differs by a factor four from the value obtained by Van de Moesdijk at 60 °C. The values agree if it is assumed that for every 10 K temperature difference the reaction-rate constant decreases by a factor two.

6.5.2. Hydrogenation of 3-pentanone in water.
The hydrogenation of 3-pentanone in water was performed at 30 °C. The overall equation reads:

$$(C_2H_5)_2CO \ (aq) + H_2 \ (aq) = (C_2H_5)_2CHOH \ (aq) \qquad (6\text{-}19)$$

The hydrogenation of 2-propanone has been discussed by Lemcoff and Jameson [113] and Freund and Hulburt [114]. The hydrogenation of 2-propanone was carried out with Raney nickel as catalyst. They found that the reaction is of zero order in 2-propanone and of order a half in hydrogen.
The hydrogenation of 3-pentanone was carried out in water at 30 °C at pH = 3. The 3-pentanone concentration was 100 or 400 mol m^{-3}.
The Whitman cell was first filled with 1117 or 1080 g water which had been degassed for three hours. In part of the water the catalyst was suspended while hydrogen was led through for one hour. When the Whitman cell was filled with water, catalyst and hydrogen, 9.8 or 39 g 3-pentanone was injected into the liquid phase. The stopwatch was started and the gas absorption was measured by recording the absorbed volume of gas every minute.
The volume of liquid in the cell was 1134 ml, giving an interfacial area of about 8.7 m^{-1}. As catalyst we used a 5 wt % Pt/C catalyst (Drijfhout). The particle diameter distribution is given in Fig. 6.4. The number-average particle diameter is 3.0 μm.
The density of the porous particles is 399 kg m^{-3}; the density of the solid itself is 1921 kg m^{-3}, resulting in a porosity of 0.79. The pores volume is $2\ 10^{-3}$ m^3 kg^{-1}. The specific surface area of this catalyst is $811\ 10^3$ m^2 kg^{-1}. In Table 6.6., these values are summarized.
For the liquid-film mass transfer coefficient a value of $3.7\ 10^{-5}$ m s^{-1} was found. From Chapters 3 and 4 we find the solubility and the diffusion coefficient of hydrogen in the above-described solution to be $C_{Ai} = 0.69$ mol m^{-3} and $D = 3.6\ 10^{-9}$ m^2 s^{-1} respectively; both values refer to 30 °C and a total pressure of 1 bar. For the effective diffusion coefficient we used a value of $0.9\ 10^{-9}$ m^2 s^{-1}. This value has been calculated from the relation $D^* = D\varepsilon_p/\tau$ in which $\varepsilon_p = 0.79$ and $\tau = 3$ for carbon particles [119].
In Table 6.7., the data which we used in our calculations are summarized.

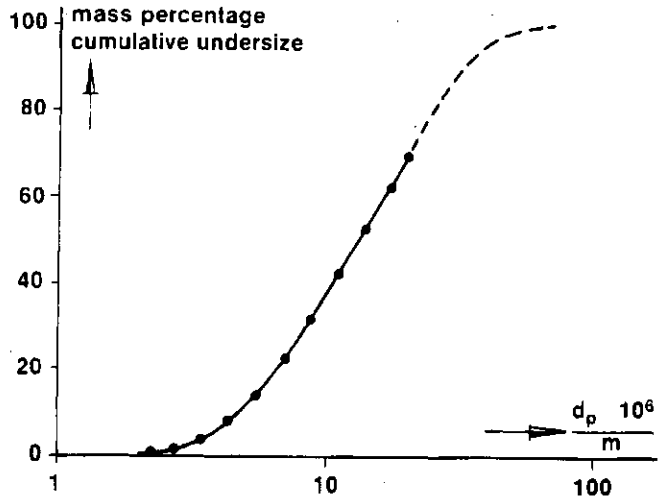

Fig. 6.4. Catalyst particle diameter distribution of 5 wt % Pt/C from Drijfhout.

Table 6.6. Properties of the 5 wt % Pt/C catalyst from Drijfhout.

d_p = 3.0 μm	ε_p = 0.79
ρ_p = 399 kg m^{-3}	V_p = 2 10^{-3} m^3 kg^{-1}
ρ_s = 1921 kg m^{-3}	S_p = 811 10^3 m^2 kg^{-1}
	δ_p = 10 nm

Table 6.7. Properties of the system hydrogen/aqueous 3-pentanone solution at 30 °C and at about 1 bar total pressure in the Whitman cell.

k_L = 3.7 10^{-5} m s^{-1}	C_{Ai} = 0.69 mol m^{-3}
D = 3.6 10^{-9} m^2 s^{-1}	a_L = 8.7 m^{-1}
D* = 0.9 10^{-9} m^2 s^{-1}	

In Table 6.8., the experimental results of the hydrogenation of 3-pentanone in water are given.
The enhancement factor has been calculated from $\Phi_A/(k_L a_L C_{Ai})$.
It was found that the reaction was of zero order in 3-pentanone. Further, it is obvious that for a large number of experiments E > 2. Table 6.8. shows that $\phi' = \phi''$ because of the small value of $a_L\delta$
It is interesting to note that after injection of 3-pentanone into the liquid phase of the Whitman cell we visually observed that the catalyst particles preferred to stay in the neighbourhood of the gas-liquid interface despite intensive stirring of the liquid.

Table 6.8. Experimental results of the hydrogenation of 3-pentanone in water at 30 °C and at about 1 bar total pressure.

Exp. No.	$\Phi_A\ 10^3$	E	$\bar{C}_p$	C_B	$\phi'\ 10^3$	ϕ	$\phi''\ 10^3$
	mol m^{-3} s^{-1}		kg m^{-3}	mol m^{-3}			
6-7	0.20	0.8	0.02	400	0.05	0.06	0.05
6-8	0.21	0.9	0.03	440	0.08	0.09	0.08
6-9	0.24	1.1	0.04	440	0.10	0.12	0.10
6-10	0.39	1.8	0.06	100	0.15	0.18	0.15
6-11	0.45	2.0	0.09	400	0.23	0.27	0.23
6-12	0.94	3.8	0.11	400	0.28	0.33	0.28
6-13	0.97	4.4	0.16	100	0.40	0.47	0.40
6-14	1.17	5.3	0.28	100	0.70	0.83	0.70
6-15	1.42	6.4	0.87	100	2.18	2.58	2.18
6-16	1.64	7.4	1.13	100	2.83	3.35	2.83
6-17	2.43	11.0	1.77	100	4.44	5.24	4.44

Model 1: reaction in the bulk of the liquid only.

This model was not applied to the experimental results of Table 6.8. since $E > 1$ for most of the experiments.

Model 2: reaction in the liquid film only.

From eqn (5-126) and Table 5.1., it is found that if $E > 2$:

$$E = Ha_{\frac{1}{2}}\phi^{\frac{1}{2}} = \Theta_{\frac{1}{2}} \qquad (6\text{-}20)$$

From eqn (5-123), the Hatta number for $n = \frac{1}{2}$ and $m = 0$ reads:

$$Ha_{\frac{1}{2}} = (1/k_L)\{4k_{\frac{1}{2}}D/(3C_{Ai}^{\frac{1}{2}})\}^{\frac{1}{2}} \qquad (6\text{-}21)$$

For the above-mentioned conditions, the Hatta number is:

$$Ha_{\frac{1}{2}} = C_{17}\ k_{\frac{1}{2}}^{\frac{1}{2}} \qquad (6\text{-}22)$$

in which:

$$C_{17} = 2.05\ mol^{-0.5}\ m^{1.5}\ s \qquad (6\text{-}23)$$

so that:

$$E = C_{17}\ (k_{\frac{1}{2}}\phi)^{\frac{1}{2}} \qquad (6\text{-}24)$$

From a plot of E versus $\phi^{\frac{1}{2}}$, see Fig. 6.5., it is found that:

$$k_{\frac{1}{2}} = 5.1\ mol^{0.5}\ m^{-1.5}\ s^{-1} \qquad (6\text{-}25)$$

for the experiments 6-11 to 6-17.
With the result of eqn (6-25), values of $\Theta_{\frac{1}{2}}$ and E can be calculated. The experimental and calculated enhancement factors are given in Table 6.9.
In Fig. 6.5. the experimentally determined points as well as the best-fit line representing the enhancement factor are given.

Table 6.9. Experimental and calculated enhancement factors for the hydrogenation of 3-pentanone in water at 30 °C and at a total pressure of about 1 bar.

Exp. No.	E_{exp}	E_{calc}	$\theta_{1/2}$
6-11	2.0	2.4	2.4
6-12	3.8	2.6	2.6
6-13	4.4	3.2	3.2
6-14	5.3	4.2	4.2
6-15	6.4	7.4	7.4
6-16	7.4	8.4	8.4
6-17	11.0	10.6	10.6

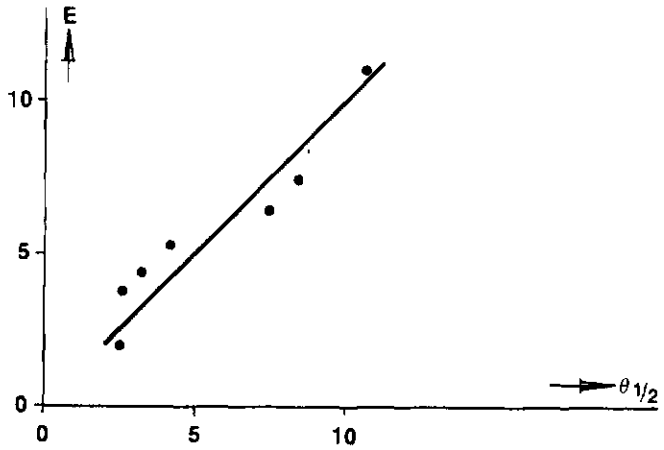

Fig. 6.5. Experimentally determined points and the calculated best-fit line (eqn (6-20)) representing the enhancement factor as a function of $\theta_{1/2}$ for the hydrogenation of 3-pentanone in water at 30 °C and at a total pressure of about 1 bar (Model 2).

Model 3: reaction in the liquid film and in the bulk of the liquid.

For $E > 2$ the same relations are obtained for Model 3 and for Model 2. Therefore, similar results may be expected.

6.5.3. Hydrogenation of styrene in n-heptane.
The hydrogenation of α-methylstyrene has been discussed by several investigators [14,18,115,116].
It was found that the reaction was of first order in hydrogen and of zero order in α-methylstyrene.
In the present work the hydrogenation of styrene was carried out in the Whitman cell at 30 °C in n-heptane, indicated by (h):

$$C_6H_5(C_2H_3)\ (h) + H_2\ (h) = C_6H_5(C_2H_5)\ (h) \qquad (6\text{-}26)$$

This hydrogenation too is of zero order in styrene and of first order in hydrogen. The concentration of styrene was 210 or 410 mol m^{-3}.
Since a new Whitman cell was used whose dimensions differed a little from those

of the cell used for the experiments described in the foregoing sections, the specific interfacial area was somewhat larger: 9.6 m^{-1}.
As catalyst we again used the 10 wt % Pd/C catalyst from Fluka. The data of this catalyst have already been given in Table 6.1.
The liquid-film mass transfer coefficient has a value of $6.7\ 10^{-4}$ m s^{-1}. The diffusion coefficient was determined according to the method described in Chapter 4 and was found to be $13\ 10^{-9}$ m^2 s^{-1}. For the effective diffusion coefficient of hydrogen in the pores of the particles we obtained a value of $3.4\ 10^{-9}$ m^2 s^{-1} after substitution of $\epsilon_p = 0.8$ and $\tau = 3$ in the relation $D^* = D\epsilon_p/\tau$ [119]. The solubility of hydrogen in the reaction liquid was assumed to be equal to that of hydrogen in n-heptane. The value of 4.8 mol m^{-3} at a total pressure of 1 bar and at 30 °C was used in our calculations.
In Table 6.10., the physical data of the reaction system used in our calculations are presented.

Table 6.10. Properties of the system hydrogen/styrene solution in n-heptane at 30 °C and at about 1 bar total pressure in the Whitman cell.

$k_L = 6.7\ 10^{-4}$ m s^{-1}
$D = 13\ 10^{-9}$ m^2 s^{-1}
$D^* = 3.4\ 10^{-9}$ m^2 s^{-1}

$C_{Ai} = 4.8$ mol m^{-3}
$a_L = 9.6$ m^{-1}

In Table 6.11., the experimental data of the hydrogenation of styrene in n-heptane are given.

Table 6.11. Experimental results of the hydrogenation of styrene in n-heptane at 30 °C and at about 1 bar total pressure.

Exp. No.	$\Phi_A\ 10^3$	E	$\overline{C}_p$	C_B	$\phi'\ 10^3$	φ	$\phi''\ 10^3$
	mol m^{-3} s^{-1}		kg m^{-3}	mol m^{-3}			
6-18	6.9	0.22	0.03	210	0.07	0.40	0.07
6-19	7.0	0.23	0.02	210	0.05	0.27	0.05
6-20	11.3	0.37	0.07	210	0.17	0.93	0.17
6-21	12.9	0.42	0.09	210	0.22	1.19	0.22
6-22	17.9	0.58	0.29	210	0.72	3.84	0.72
6-23	20.0	0.65	0.15	210	0.37	1.99	0.37
6-24	20.0	0.65	0.39	210	0.96	5.17	0.96
6-25	20.4	0.66	0.11	210	0.27	1.46	0.27
6-26	22.1	0.72	0.49	210	1.21	6.50	1.21
6-27	22.3	0.72	0.29	210	0.72	3.84	0.72
6-28	24.4	0.79	0.97	210	2.40	12.86	2.40
6-29	27.2	0.88	1.92	410	4.74	25.45	4.74
6-30	28.4	0.92	1.44	210	3.56	19.09	3.56
6-31	29.6	0.96	1.93	210	4.77	25.58	4.77
6-32	31.6	1.02	3.86	210	9.53	51.17	9.53

Table 6.11. shows that $\phi' = \phi''$ because of the small value of $a_L\delta$. The enhancement factor is calculated from $\Phi_A/(k_L a_L C_{Ai})$. Further we visually

observed that the catalyst particles were dispersed homogeneously in the reaction system.

Model 1: reaction in the bulk of the liquid only.

From eqn (5-45) and Table 5.1., it is found that:

$$1/E = 1 + (1 - a_L\delta)/(\eta_l\Theta_l^2) + 1/\Gamma' = 1 + (1 - a_L\delta)/(\eta_l Ha_l^2\phi) + 1/\Gamma' \quad (6\text{-}27)$$

For the above-described conditions, the Hatta number is:

$$Ha_l^2 = C_{18}\, k_l \quad (6\text{-}28)$$

in which:

$$C_{18} = 0.03\ s \quad (6\text{-}29)$$

so that:

$$\Theta_l^2 = C_{18}\, k_l\phi \quad (6\text{-}30)$$

From a plot of $(1/E - 1 - 1/\Gamma')$ versus $(1/\phi)$ we can calculate k_l. Assuming $Sh_p > 2$, $D = 13\ 10^{-9}\ m^2\ s^{-1}$ and $d_p = 4\ 10^{-6}$ m, we obtain:

$$k_s > 6.5\ 10^{-3}\ m\ s^{-1} \quad (6\text{-}31)$$

Combination of the eqns (5-18) and (6-31) leads to:

$$\Gamma' > C_{19}\, \overline{C}_p \quad (6\text{-}32)$$

in which:

$$C_{19} = 3.7\ 10^3\ m^3\ kg^{-1} \quad (6\text{-}33)$$

Substitution of the smallest value of $\overline{C}_p$ mentioned in Table 6.11. in eqn (6-32) gives a minimum value of 75 for Γ', provided that the catalyst particles have been dispersed completely.
Since $1/\Gamma' \ll 1$, we may neglect the contribution of $1/\Gamma'$ in eqn (6-27). As a consequence:

$$1/E - 1 = \{(1 - a_L\delta)/(\eta_l Ha_l^2)\}(1/\phi) \quad (6\text{-}34)$$

From the plot of $(1/E - 1)$ versus $(1/\phi)$ we determined k_l with the data represented in Table 6.11., assuming $\eta_l = 1$:

$$k_l = 32\ s^{-1} \quad (6\text{-}35)$$

With the result of eqn (6-35), it appeared that the effectiveness of the catalyst particles is unity. In Table 6.12., the experimental and calculated enhancement factors are presented. In Fig. 6.6., the experimentally determined points and the calculated best-fit curve representing the enhancement factor are given.

Model 2: reaction in the liquid film only.

This model was not applied to the experimental results of Table 6.11. since it was visually observed that the catalyst particles were present in the bulk of the liquid too.

Model 3: reaction in the liquid film and in the bulk of the liquid.

For this model we must apply eqn (5-115) to the experimental results. Again $Ha_1^2 = C_{18}\, k_1$ and $\Theta_1^2 = Ha_1^2\phi$. From eqn (5-116) it is found that:

$$\lambda''\delta = (a_L\delta)^{\frac{1}{2}}\Theta_1 = (a_L\delta)^{\frac{1}{2}}Ha_1 c^{\frac{1}{2}} = C_{20}\,(k_1\phi)^{\frac{1}{2}} \qquad (6\text{-}36)$$

in which:

$$C_{20} = 4\ 10^{-4}\ s^{\frac{1}{2}} \qquad (6\text{-}37)$$

The effectiveness is assumed to be unity. The term Θ_1^2/Γ follows from:

$$\Theta_1^2/\Gamma = k_1 d_p/(6k_s) \qquad (6\text{-}38)$$

Sustituting $k_1 = 25\ s^{-1}$, $d_p = 4\ 10^{-6}$ m and $k_s \geq 6.5\ 10^{-3}$ m s^{-1} in eqn (6-38), we calculated that:

$$\Theta_1^2/\Gamma \leq 2.5\ 10^{-3} \qquad (6\text{-}39)$$

As a consequence, the term Θ_1^2/Γ in eqn (5-115) is neglected. When applying the least-squares method, it is found that:

$$k_1 = 22\ s^{-1} \qquad (6\text{-}40)$$

The result of eqn (6-40) confirms that the effectiveness of the catalyst particles is unity. In Table 6.12., the experimental and calculated enhancement factors are presented, while in Fig. 6.7. a graphical representation is given. It can be seen from Figs. 6.6. and 6.7. that Model 3 describes the experimental results of Table 6.11. better than Model 1. The same conclusion can be drawn when comparing the minimum value of $\sum(E_{exp} - E_{calc})^2$ for both models; this minimum value is 0.10 for Model 3 and 0.15 for Model 1.

Table 6.12. Experimental and calculated enhancement factors for the hydrogenation of styrene in n-heptane at 30 °C and at a total pressure of about 1 bar.

		Model 1		Model 3	
Exp. No.	E_{exp}	E_{calc}	$\Theta_1^2/(1 - a_L\delta)$	E_{calc}	$\Theta_1^2/(1 - a_L\delta)$
6-18	0.22	0.27	0.37	0.21	0.26
6-19	0.23	0.19	0.24	0.15	0.17
6-20	0.37	0.46	0.85	0.38	0.60
6-21	0.42	0.50	1.00	0.44	0.77
6-22	0.58	0.78	3.53	0.71	2.50
6-23	0.65	0.65	1.82	0.56	1.29
6-24	0.65	0.83	4.74	0.77	3.36
6-25	0.66	0.57	1.34	0.49	0.95
6-26	0.72	0.86	5.96	0.81	4.22
6-27	0.72	0.78	3.53	0.71	2.50
6-28	0.79	0.92	11.79	0.89	8.36
6-29	0.88	0.96	23.33	0.94	16.54
6-30	0.92	0.95	17.50	0.93	12.40
6-31	0.96	0.96	23.45	0.94	16.62
6-32	1.02	----	-----	0.97	33.24

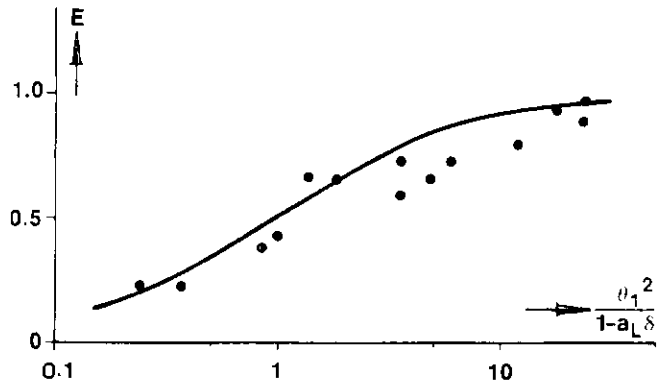

Fig. 6.6. Experimentally determined points and the calculated best-fit curve (eqn (6-27)) representing the enhancement factor as a function of $\Theta_1^2/(1 - a_L\delta)$ for the hydrogenation of styrene in n-heptane at 30 °C and at a total pressure of about 1 bar (Model 1).

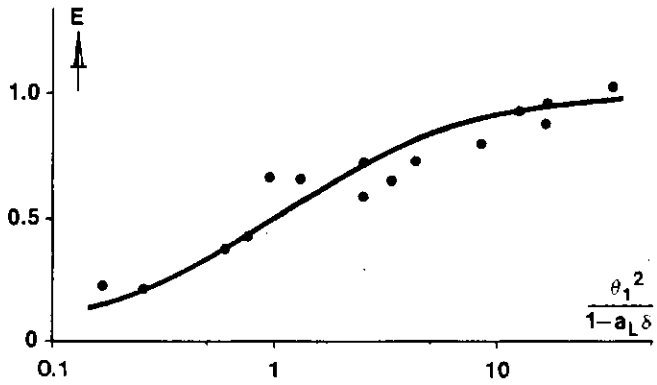

Fig. 6.7. Experimentally determined points and the calculated best-fit curve (eqn (5-115)) representing the enhancement factor as a function of $\Theta_1^2/(1 - a_L\delta)$ for the hydrogenation of styrene in n-heptane at 30 °C and at a total pressure of about 1 bar (Model 3).

6.6. Conclusions.

In this chapter we have shown that the gas absorption rate in a heterogeneously catalyzed chemical reaction system can be described by three models developed in Chapter 5. Which model has to be applied to experimental results carried out with a slurry reactor is dependent on the size of the catalyst particles and the tendency of the particles to stay in the film near the gas-liquid interface or in the bulk of the liquid.

If the liquid film near the gas-liquid interface contains sufficient small catalyst particles and the reaction rate is sufficiently high, an enhancement factor larger than unity may be expected, in particular if k_L is relatively small as is the case for very small gas bubbles.

CHAPTER 7

DESIGN OF SLURRY REACTORS

7.1. Physical quantities and relations.

In the design of slurry reactors, the rate of conversion plays an important role in the dimensioning of the reactor. The rate of conversion depends on the mass transfer rate, the kinetics of the reaction, the catalyst concentration and other process conditions. Moreover, in most of the reactions heat transfer must be taken into account in the design of the reactor.
The subject of heat transfer has not been dealt with in this thesis. Some work on heat transfer in bubble columns has been done by Kölbel et al. [7] and Hikita et al. [117].
In this work we have treated the mass transfer in slurry reactors in which components react on the active sites of solid catalyst particles. One of the reacting components is a gas absorbed from a dispersed gas phase into the liquid phase. The other component is dissolved in the continuous liquid phase. This chapter deals with the design of slurry reactors.
Therefore, we need reliable values of:
- transport properties of the gas-liquid system: D, η, σ, He, ρ;
- transport coefficients of the gas-liquid system: k_L, k_G, k_s;
- process conditions: u_G, u_L, H_0, T, d_s, ε, a_L, a_s, C_B, p_A, T', $\overline{C}_p$;
- kinetics: k_n, n, m;
- catalyst properties: d_p, ε_p, ρ_p, S_p, V_p, τ.

For a reliable design it is required to use values of the properties measured under the same operating conditions as used in the reactor, for instance with respect to temperature, pressure, and composition of the reaction system.
We have shown how reliable values of the above-mentioned properties can be obtained. These values can be used for the design of a slurry reactor.
The aim of the procedure in this chapter is to calculate the production capacity of a given reactor and reaction system or to determine the volume of a reactor required to achieve a particular production rate.
The first step is to plot the enhancement factor E versus the modified Hatta number Θ_n, as done in Chapter 5. In Chapter 5 three models were given for the mass transfer of gas from the gas phase to the active sites of the catalyst particles suspended in the liquid phase. It is obvious that the most conservative value of E is obtained when we assume that the catalyst particles are in the bulk of the liquid only. We have derived only the equations in which the reaction rate is of zero order or first order in the gas component. Equations referring to other orders should be treated in the same way. This means that the reaction orders n and m must be known.
To obtain a reliable correlation between E and Θ_n, measurements must be performed in, for example, a Whitman cell.
In the Whitman cell we have to determine:

$$E = \Phi_A/(k_L a_L C_{Ai}) \tag{7-1}$$

$$\Theta_n = (1/k_L)\{2k_n C_{Ai}^{n-1} C_B^m D\phi/(n+1)\}^{\frac{1}{2}} = Ha_n \phi^{\frac{1}{2}} \tag{7-2}$$

$$\Gamma = k_s a_s/(k_L a_L) \tag{7-3a}$$

$$\text{or } \Gamma' = k_s a_s/(k_L a_L(1 - a_L\delta)) \tag{7-3b}$$

$$\Lambda_n = k_n C_B^m C_{Ai}^{n-1} d_p^2 (n+1)/(24D^*) \tag{7-4}$$

$$\phi = \overline{C}_p/(\rho_p a_L \delta) \tag{7-5a}$$

$$\text{or } \phi' = \overline{C}_p/(\rho_p(1 - a_L\delta)) \tag{7-5b}$$

or $\phi'' = \overline{C}_p/\rho_p$ (7-5c)

Φ_A, k_n, n and m are determined experimentally from the absorption rate if chemical reaction occurs. The values of C_B and $\overline{C}_p$ are calculated from the number of moles or mass added to the cell per unit volume of liquid.
The value of a_L for a Whitman cell can be calculated from:

$$a_L = \frac{\pi D_w^2}{4V_L} \qquad (7\text{-}6)$$

The value of a_s follows from:

$$a_s = 6\overline{C}_p/(\rho_p d_p) \text{ or } a_s = 6\phi''/d_p \qquad (7\text{-}7)$$

The value of k_L is calculated from the experiments in which no chemical reaction takes place.
If catalyst particles are used, the catalyst support should be dispersed in the reaction medium. In Chapter 6 we described how to perform these experiments.
If these experiments are to be carried out under pressure and at high temperatures, an autoclave must be used.
It should be pointed out that the gas absorption rate both with and without chemical reaction is determined under identical conditions with respect to temperature, pressure, geometry of the reactor, stirrer speed and composition of the three phases.
Furthermore, knowledge of some properties of the catalyst and the reaction system is needed to be able to plot E versus Θ_n.
The values of ε_p, d_p, τ and ρ_p are determined according to methods well-known in catalysis.
The value of the effective diffusion coefficient is calculated from $D^* = D\varepsilon_p/\tau$.
In Chapter 4 we described a method to determine reliable and accurate values of the diffusion coefficient D of slightly soluble gases in liquids.
The solubility of the gas in the liquid medium is determined by the method given in section 3.7. The use of a stream of liquid in a gas-liquid system enables rapid and accurate determination of the Henry number He.
The measurement of the diffusion coefficient and Henry number can be carried out under pressure when the equipment presented in this thesis is modified.
With the data obtained in this way E can be plotted versus Θ_n on the basis of experiments in the Whitman cell.

When translating the results obtained with the Whitman cell to the commercial reactor it should be borne in mind that the values of some physical quantities will not change if the reactor is operated under the same conditions of temperature, pressure, and composition of the reaction system as used in the Whitman cell.
The unchanged properties are:
- transport properties D, η, σ, ρ and He;
- kinetic constants k_n, n and m;
- catalyst properties d_p, ε_p, ρ_p, S_p, V_p, τ and μ.

In Chapter 2 we described experiments in a bubble column investigating the influence of u_G on d_s, a_L and ε_{av}. These experiments were performed in a bubble column with a diameter T = 29 cm. This relatively large diameter has been chosen to minimize the influence of the wall. Furthermore, the middle section of the dispersion in the column must be large compared with on-stream zone and foam layer.
From the experiments in Chapter 2 it may be concluded that reliable data can be obtained only if the experiments are carried out with a dispersion of representative composition.

For small bubbles ($d_s < 0.5$ mm) in the field of gravity the value of k_L is almost independent of the process conditions and is mainly determined by the physical properties of the reaction system [37-40]. For calculation of the mass transfer coefficient, knowledge of ρ, η and D is needed. Further, the surface tension gradient can influence k_L (Marangoni-effect) [118].
At the gas-liquid interface, mass transfer resistance in the gas film is almost negligible in comparison with that in the liquid film.
Values of k_s can be approximated by $Sh_p = 2$.
Further, the value of a_L must be known under commercial reaction conditions:

$$a_L = 6\varepsilon_{av}/d_s \qquad (7\text{-}9)$$

Therefore, values of ε_{av} and d_s must be determined. From Chapter 2 it is known that d_s is almost constant under the normal process conditions we investigated. In sections 2.2.5 and 2.2.7 we described how the Sauter mean diameter d_s can be determined by:
- chemical method [9,41,49];
- photographic method [9,38,40,41];
- resistivity probe method [56,57];
- gas disengagement method [67];
- correlations [9,10,40,45].

The disadvantage of the photographic method is that it cannot be applied to slurries of small carbon particles. When proper precautions are taken, all methods can also be used for systems under pressure.

The average gas holdup ε_{av} must be determined experimentally. This can be done by visual observation if the vessel is made of a transparant material and its diameter $T > 0.3$ m. For high pressures the column must have a sight-glass or must be equipped with a float.
The relation between the average gas holdup and the superficial gas velocity can be represented by:

$$1/\varepsilon_{av} = b + v_o/u_G;\ b > 1 \qquad (7\text{-}10)$$

As a consequence, the specific interfacial area is given by:

$$a_L = 6u_G\{(v_o + bu_G)d_s\}^{-1} \qquad (7\text{-}11)$$

If reliable values of the physical properties are available ε_{av} can be calculated from correlations presented in the literature (see Table 2.1.).
These correlations may be used only within a given range of process conditions and transport properties.
The effect of the superficial liquid velocity and the ratio of the clear liquid height to the column diameter on the average gas holdup is mostly negligible if the superficial gas velocity remains unchanged.
Finally, the values of $\bar{C}_p$ and C_B can be chosen and the value of a_s be calculated.
With the values of the various parameters it is possible to calculate Θ_n as well as other dimensionless numbers. With this information both E and Φ_A can be calculated for a commercial reactor.

7.2. Influence of gas holdup and particle size on mass transfer rate.
If gas bubbles and solid particles are dispersed in a liquid, the gas volume is:

$$V_G = \varepsilon_{av}V_L/(1 - \varepsilon_{av}) \qquad (7\text{-}12)$$

The number of gas bubbles in the dispersion is given by:

$$n_b = 6V_G/(\pi d_s^3) = 6\varepsilon_{av}V_L/(\pi d_s^3(1 - \varepsilon_{av})) \qquad (7\text{-}13)$$

When there is a catalyst concentration $\overline{C}_p$, the total mass of catalyst in the dispersion equals $\overline{C}_pV_L$. The number of catalyst particles is found from:

$$n_p = 6\overline{C}_pV_L/(\pi d_p^3\rho_p) \qquad (7\text{-}14)$$

Thus the number of catalyst particles per gas bubble equals:

$$n_p^* = \overline{C}_p d_s^3(1 - \varepsilon_{av})/(d_p^3\rho_p\varepsilon_{av}) \qquad (7\text{-}15)$$

Let us further consider a spherical layer of liquid (see Fig. 7.1.) with an inside diameter d_s and an outside diameter d_L which encloses a gas bubble of diameter d_s. It is clear that for this system the gas holdup is given by:

$$\varepsilon_{av} = d_s^3/d_L^3 \qquad (7\text{-}16)$$

so that

$$d_L^3 = d_s^3/\varepsilon_{av} \qquad (7\text{-}17)$$

The volume of liquid per gas bubble is calculated from eqn (7-13):

$$V_L/n_b = \pi d_s^3(1 - \varepsilon_{av})/(6\varepsilon_{av}) \qquad (7\text{-}18)$$

The thickness of the liquid film around the gas bubble is given by:

$$\delta = D/k_L \qquad (7\text{-}19)$$

The volume of the liquid film per gas bubble equals:

$$V_F/n_b = \pi\{(d_s + 2\delta)^3 - d_s^3\}/6 \qquad (7\text{-}20)$$

so that the ratio of liquid film volume to liquid volume is calculated from:

$$V_F/V_L = \{(d_s + 2\delta)^3 - d_s^3\}\varepsilon_{av}/\{d_s^3(1 - \varepsilon_{av})\} \qquad (7\text{-}21)$$

The number of catalyst particles in the liquid film per gas bubble equals:

$$n_p^o = \overline{C}_p\{(d_s + 2\delta)^3 - d_s^3\}/(\rho_p d_p^3) \qquad (7\text{-}22)$$

assuming that the catalyst particles are divided homogeneously between bulk of the liquid and liquid film.
When the catalyst particles are assumed to be in the liquid film only, the concentration of the catalyst in the liquid film is given by:

$$C_p^o = \overline{C}_p d_s^3(1 - \varepsilon_{av})/\{\{(d_s + 2\delta)^3 - d_s^3\}\varepsilon_{av}\} \qquad (7\text{-}23)$$

In the following we will show the influence of gas holdup and catalyst particle size on mass transfer rate by means of two examples.

Example 1.

Let us consider the following conditions:

$\varepsilon_{av} = 0.2$
$d_s = 200\ \mu m$
$d_p = 100\ \mu m$
$\overline{C}_p = 12.5\ kg\ m^{-3}$
$\rho_p = 400\ kg\ m^{-3}$
$D = 5\ 10^{-9}\ m^2\ s^{-1}$
$k_L = 10^{-4}\ m\ s^{-1}$

With these conditions we calculated:

$n_p^* = 1$
$d_L = 342\ \mu m$
$\delta = 50\ \mu m$
$n_p^o = 0.6$
$V_F/V_L = 0.6$

This situation is represented in Fig. 7.1.

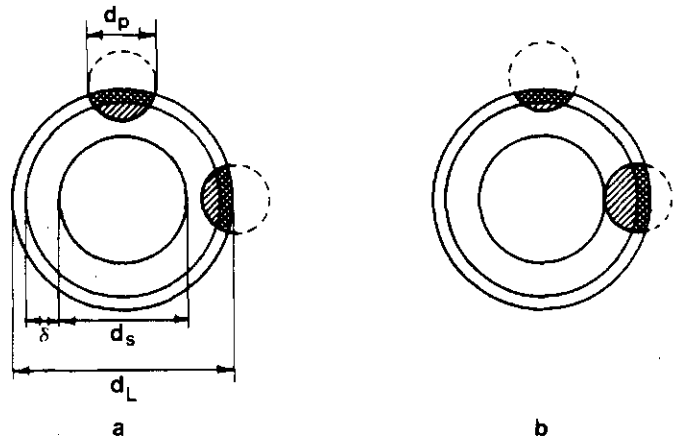

Fig. 7.1. Representation of one gas bubble in a slurry for the conditions of example 1; $n_p^* = 1$ i.e. one catalyst particle per gas bubble.

In Fig. 7.1a. we have drawn two catalyst particles. Both catalyst particles are positioned identically. The total catalyst volume per gas bubble equals that of one catalyst particle. The total catalyst volume in the liquid film is about 0.6 times that of one catalyst particle.
In Fig. 7.1b. n_p^* and n_p^o have the same values as above. In Fig. 7.1b. we placed one catalyst particle adjacent to the gas bubble so that a larger part of that catalyst particle is in the liquid film. To obey the condition of $n_p^o = 0.6$, the other catalyst particle is placed further from the gas bubble.

Example 2.

The conditions are identical with those of Example 1 except for the catalyst diameter:

$d_p = 10\ \mu m$.

We calculated the following values:

$n_p^* = 1000$
$d_L = 342\ \mu m$
$n_p^o = 594$
$V_F/V_L = 0.594$
$\delta = 50\ \mu m$
$C_p^o = 21\ kg\ m^{-3}$

In Fig. 7.2a. we have drawn the situation in which the catalyst particles are distributed homogeneously between liquid film and bulk of the liquid.
In making these drawings it was assumed that the depth of the cross-sectional view equals d_p.
The number of catalyst particles in this cross-sectional view can be obtained from:

$$n_c = 3d_p(d_L^2 - d_s^2)n_p^*/\{2(d_L^3 - d_s^3)\} \qquad (7\text{-}24)$$

If each catalyst particle in bulk and film of Fig. 7.2a. is brought to the gas-liquid interface, the gas-liquid interface area occupied by catalyst particles can be obtained by projection of these particles on the surface of the bubble. Consequently, the fraction of the gas bubble surface occupied by catalyst particles can be approximated by:

$$f_o = n_p^* d_p^2/(4d_s^2) = \overline{c}_p d_s(1 - \varepsilon_{av})/(4d_p\rho_p\varepsilon_{av}) \qquad (7\text{-}25)$$

In this case it is assumed that all particles form a monolayer of catalyst particles along the surface of the gas bubble.
For the conditions given, we found $f_o = 0.6$ from eqn (7-25).

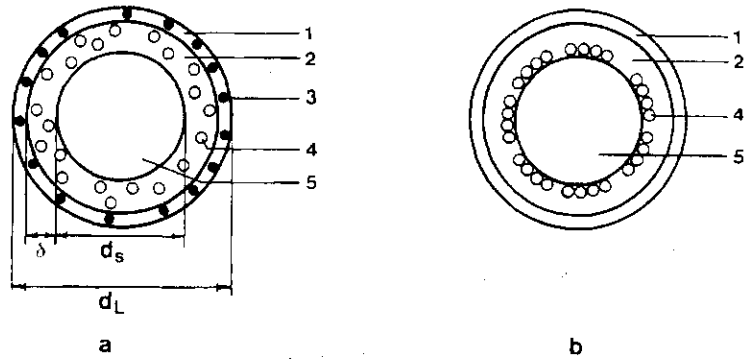

Fig. 7.2. Representation of one gas bubble in a slurry for the conditions of example 2.

1. bulk liquid
2. film liquid
3. catalyst particle in bulk liquid
4. catalyst particle in film liquid
5. gas bubble

When we compare the situation as given in Fig. 7.1. with that of Fig. 7.2a. we can conclude that the enhancement of gas absorption to be expected for the situation of Fig. 7.2a. is much higher than that for the situation of Fig. 7.1. The larger value of the enhancement factor in the situation of Fig. 7.2a. at the same catalyst concentration is caused by the smaller particle diameter and the larger number of catalyst particles near the gas bubble surface.
If we assume that the active sites are distributed homogeneously in the catalyst particles, independent of the particle size, then the active sites are distributed more homogeneously in the liquid owing to the larger number of particles and the smaller particle diameter. This simply means that in the liquid film near the gas-liquid interface where the gas concentration is high compared with that in the bulk, more active sites are present.
The maximum yield for the given catalyst concentration and size is obtained when the particles are all pushed against the gas-bubble surface as is done in Fig. 7.2b. Here, all available active sites are in contact with the highest

possible gas concentration. Therefore, the situation in Fig. 7.2b. will give a higher gas absorption rate than the situation of Fig. 7.2a.
Generally, we can increase the fraction of occupation by increasing the catalyst concentration or by decreasing the catalyst diameter at a given gas holdup (see eqn (7-25)). The average gas holdup ε_{av} can be influenced by the superficial gas velocity. The gas bubble diameter d_s in a given reaction medium remains almost constant as we have shown in this thesis.

7.3. Summary and conclusions.
In the first part of this chapter we have mentioned the physical quantities of which the values must be known to be able to design three-phase slurry reactors. Further, we have indicated how to obtain accurate and reliable values of various hydrodynamic, kinetic and transport properties.
In the second part we paid attention to the influence of gas holdup and concentration and size of the catalyst particles on the gas absorption rate in a slurry reactor.

For a given system in a slurry reactor, the conversion of gas per unit volume of liquid can be enlarged by increasing a_L, k_L, C_{Ai} and E.
The value of $a_L = 6\varepsilon_{av}/d_s$ can primarily be influenced by the gas holdup $\varepsilon_{av} = u_G/(v_o + bu_G)$ since the bubble diameter remains almost constant.
The value of k_L can hardly be influenced, whereas the value of C_{Ai} can only be increased by increasing the partial pressure of the gas component in the gas phase.
The value of the enhancement factor is dependent on the concentration and size of the catalyst particles. Further, the value of E increases with the number of catalyst particles present in the liquid film near the gas-liquid interface in the slurry reactor.
Therefore, the values of ε_{av}, $\overline{C}_p$ and d_p must be chosen in a proper way which is dependent on the transport properties and the kinetics of the reaction system.